The role of unconventional stacking interactions on the supramolecular assemblies of Hg(II) coordination compounds

Ghodrat Mahmoudi,[a]* Antonio Bauzá,[b] Atash V. Gurbanov,[c] Fedor I. Zubkov,[d] Waldemar Maniukiewicz,[e] Antonio Rodríguez-Diéguez,[f] Elena López Torres[g] and Antonio Frontera,[b]*

[a]*Department of Chemistry, Faculty of Science, University of Maragheh, P.O. Box 55181-83111, Maragheh, Iran; E-mail: mahmoudi_ghodrat@yahoo.co.uk*

[b]*Departamento de Quimica, Universitat de les IllesBalears, Crta. de Valldemossa km 7.5, 07122 Palma de Mallorca (Baleares), Spain; E-mail: toni.frontera@uib.es*

[c]*Department of Chemistry, Baku State University, Z. Xalilov Str. 23, Az 1148 Baku, Azerbaijan.*

[d]*Department of Organic Chemistry, Peoples' Friendship University of Russia, 6 Miklukho-Maklaya St., Moscow, Russian Federation.*

[e]*Institute of General and Ecological Chemistry, Faculty of Chemistry, Lodz University of Technology, Żeromskiego 116, 90-924 Łódź, Poland.*

[f]*Department of Inorganic Chemistry, University of Granada, Avda Fuentenueva s/n, 18071, Granada, Spain.*

[g]*Departamento de Química Inorgánica, Facultad de Ciencias, Módulo 07, Universidad Autónoma de Madrid , Ctra. de Colmenar Viejo, Km 15 , 28049 Madrid, Spain.*

Table of contents:

1. Table S1:

Table S1. Crystallographic Data for compounds **1** – **9**.

Compound	**1**	**2**	**3**	**4**	**5**
chemical formula	$C_{48}H_{40}N_{16}O_4Cl_8Hg_4$	$C_{12}H_{10}N_4OBr_2Hg$	$C_{12}H_{10}N_4OI_2Hg$	$C_{13}H_{12}N_4OCl_2Hg$	$C_{13}H_{12}N_4OBr_2Hg$
M/gmol^{-1}	1990.92	586.65	680.63	511.76	600.68
T (K)	296	100	100	293	190
λ/Å	0.71073	0.71073	0.71073	0.71073	0.71073
cryst syst	monoclinic	monoclinic	monoclinic	monoclinic	monoclinic
space group	$P2_1/c$	*P21/n*	*P21/n*	*P21/n*	*P21/n*
a/ Å	7.8020(11)	7.3839(7)	7.4392(11)	7.9297(16)	8.1943(2)
b/ Å	27.364(4)	12.5740(11)	12.995(2)	13.556(3)	13.4627(2)
c/ Å	13.552(2)	15.6783(13)	16.496(3)	14.212(3)	14.4493(3)
α/ ^{o}	90	90	90	90	90
β/ ^{o}	92.062(6)	91.892(5)	94.062(2)	90.29(3)	90.865(2)
σ/ ^{o}	90	90	90	90	90
V/ Å^3	2891.4(7)	1454.9(2)	1590.7(4)	1528.8(6)	1593.83(6)
Z	2	4	4	4	4
ρ(g cm-3)	2.287	2.678	2.842	2.223	2.503
μ(mm-1)	11.015	16.072	13.558	10.419	14.674
Unique reflections	19322	2985	10942	13584	12855
R(*int*)	0.093	0.000	0.034	0.022	0.038
GOF on F^2	1.028	1.039	1.020	1.030	1.036
R1 [I > $2\sigma(I)$] [a]	0.055	0.030	0.059	0.027	0.037
wR2 [I > $2\sigma(I)$] [a]	0.129	0.057	0.145	0.054	0.064
[a] $R(F) = \sum\|\|F_o\| - \|F_c\|\|/\sum\|F_o\|$; $wR(F^2) = [\sum w(F_o^2 - F_c^2)^2/\sum wF^4]^{1/2}$					

Table S1 (cont.). Crystallographic Data for compounds **1** – **9**.

Compound	**6**	**7**	**8**	**9**
chemical formula	$C_{13}H_{14}N_4O_2I_2Hg$	$C_{18}H_{14}N_4OCl_2Hg$	$C_{18}H_{14}N_4OBr_2Hg$	$C_{18}H_{14}N_4OI_2Hg$
M/gmol^{-1}	712.67	573.82	662.74	756.72
T (K)	293	150	150	150
λ/Å	0.71073	0.71073	0.71073	0.71073
cryst syst	triclinic	triclinic	Triclinic	monoclinic
space group	*P*1	*P*-1	*P*-1	*P21/c*
a/ Å	7.6855(15)	9.2294(3)	9.3269(6)	19.9763(2)
b/ Å	7.8344(16)	11.4544(3)	11.5055(9)	11.8392(1)
c/ Å	8.1579(16)	18.2305(6)	18.7159(12)	17.7194(2)
α/ °	91.15(3)	80.471(3)	79.290(6)	90
β/ °	104.78(3)	77.234(3)	77.048(6)	103.3280(1)
σ/ °	116.81(3)	87.169(3)	86.951(6)	90
V/ Å^3	418.66(18)	1853.54(10)	1923.1(2)	4077.83(7)
Z	1	4	4	8
ρ(g cm-3)	2.827	2.056	2.289	2.465
μ(mm-1)	12.889	17.675	19.349	37.436
Unique reflections	7105	15160	14662	19906
R(*int*)	0.000	0.045	0.050	0.035
GOF on F^2	1.041	0.940	1.053	1.062
R1 [I > 2σ(*I*)] [a]	0.032	0.035	0.071	0.029
wR2 [I > 2σ(*I*)] [a]	0.079	0.090	0.1801	0.071
[a] $R(F) = \sum\|\|F_o\| - \|F_c\|\|/\sum\|F_o\|$; $wR(F^2) = [\sum w(F_o^2 - F_c^2)^2/\sum wF^4]^{1/2}$				

2. Hirshfeld surface analysis

Applying d_{norm} function to the Hirshfeld surface of **2** reveals several red areas. Two biggest of them correspond to a single hydrogen bond (C2-H2···O1) which connects complex molecules into a one-dimensional supramolecular chain. A short H···H contact (H1···H9) is present in the said chain. Another large red spot is consistent with a short C-H···C contact between aromatic rings of adjacent molecules. This in combination with four small red areas which are present due to C···C contacts indicate strong π···π stacking interactions. Weak hydrogen bonds involving bromide ions are manifested by four small red areas. They correspond to two such interactions (N3-H3···Br1 and C10-H10···Br2, Fig. S1a) which make up 30% of the Hirshfeld surface. When the surface is mapped with shape index function both red hollow areas indicating C-H···π interactions (one marked with dashed arrow on Fig. S1b) and 'bow-tie' patters (one pinpointed with plain arrow on Fig. S1b) indicating π···π interactions between pirydyl rings of adjacent complex molecules. From the analysis of decomposed (see Fig. S2) fingerprint plots one can conclude that the most important types of interactions in packing of molecules of **2** are weak hydrogen bonds in which bromide ions act as acceptors (H···Br contacts, 30.3%) and van der Waals forces (H···H contacts, 23.1%)

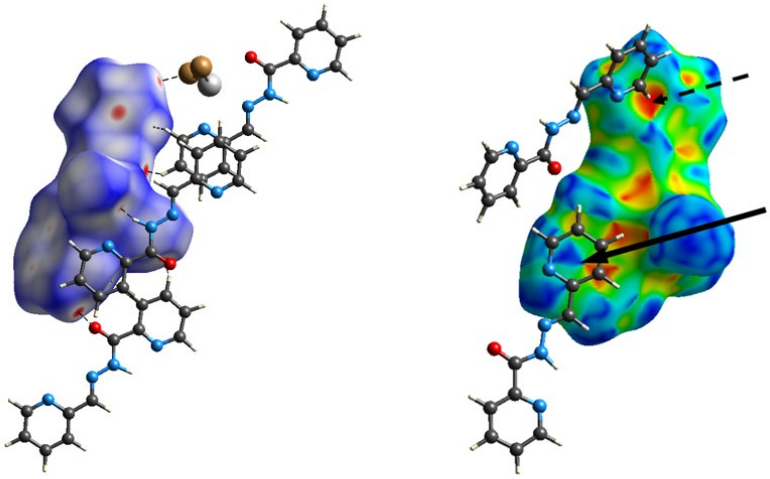

Fig. S1. Hirshfeld surface of **2** a) mapped with d_{norm} function; hydrogen bonds marked with dashed lines; b) mapped with shape index function.

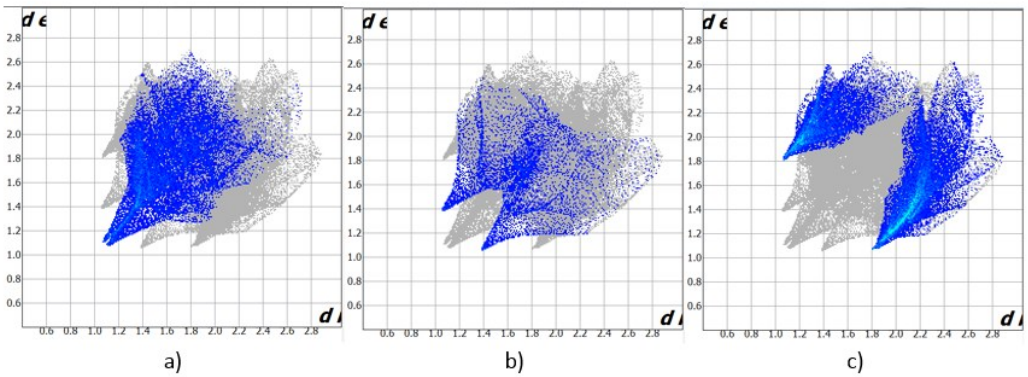

Fig. S2. Decomposed fingerprint plots of 1: a) H···H, b) H···O, c) H···Br

When Hirshfeld surface of **3** is mapped with d_{norm} function nine red spots become visible. Two biggest ones correspond to a C-H···O hydrogen bond (C10-H10···O1) which connects the molecule positioned inside the surface with two different adjacent molecules. Four small red areas are consistent with presence of two weak hydrogen bonds involving iodide ions (N1-H1A···I2 and C6-H6A···I1, Fig. S3a). There are additionally three small red spots corresponding to C···C and C-H···C contacts (C7-H7A···C7, C8···C11), which in term are consistent with 'bow-tie' patterns visible on the surface mapper with shape index function (Fig. S3b). When shape index function is applied, one can also notice red hollow areas indicating C-H···π interactions. This is also apparent when decomposed fingerprint plots are considered (Fig. S4) as H···C contacts constitute 12.5% of the surface. Typically, H···H contacts (van der Waals forces, 22.6%) and hydrogen bonds involving halogen ion (30.0%) contribute mostly to the surface.

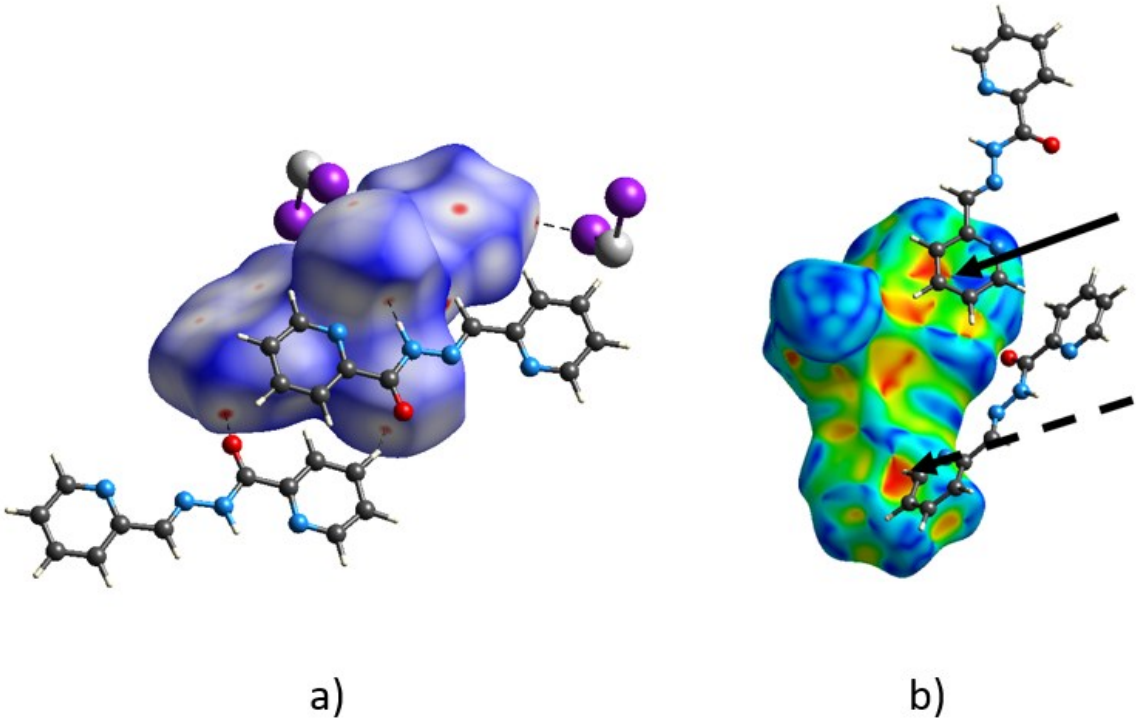

Fig. S3. Hirshfeld surface of **3** a) mapped with d_{norm} function with hydrogen bonds marked with dashed lines; b) mapped with shape index function; plain arroe marks 'bow-tie' pattern while dashed arrow indicates C-H···π interaction.

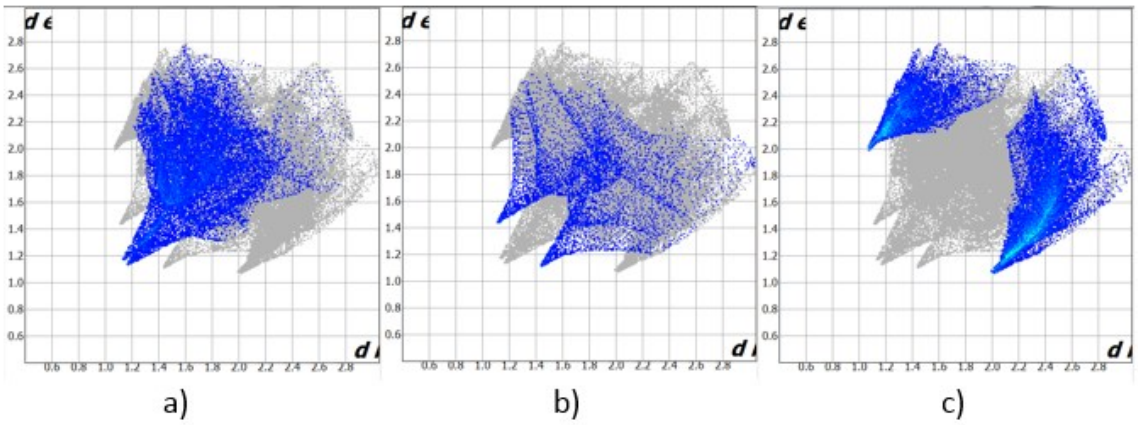

Fig. S4. Decomposed fingerprint plots of **3** a) H···H, b) H···O, c) H···I

When the Hirshfeld surface of **5** is mapped with d_{norm} function, one can notice seven red spots. Two biggest ones correspond to one C-H···O hydrogen bond (C4-H4···O1), while two additional small red areas are present due to one C-H···Br interaction (C10-H10···Br1). Three remaining red areas are consistent with one C-H···C interaction (C9-H9···C9, one) and one C···Br interaction (C3···Br2). Applying shape index function to the surface reveals the usual 'bow-tie' pattern indicative of π···π stacking (Fig. S5b). One can also notice parts of the surface of the molecule which are complementary to each other, with the hollow area in red and bulged one (around one of the bromide ions) in blue (Fig. S5b). Decomposed fingerprint plots of **5** (Fig. S6) indicate that – like with previous – compounds, the major interactions contributing to packing of molecules are van der Waals forces (H···H contacts, 26.0%) and H···Br interactions (31.2%).

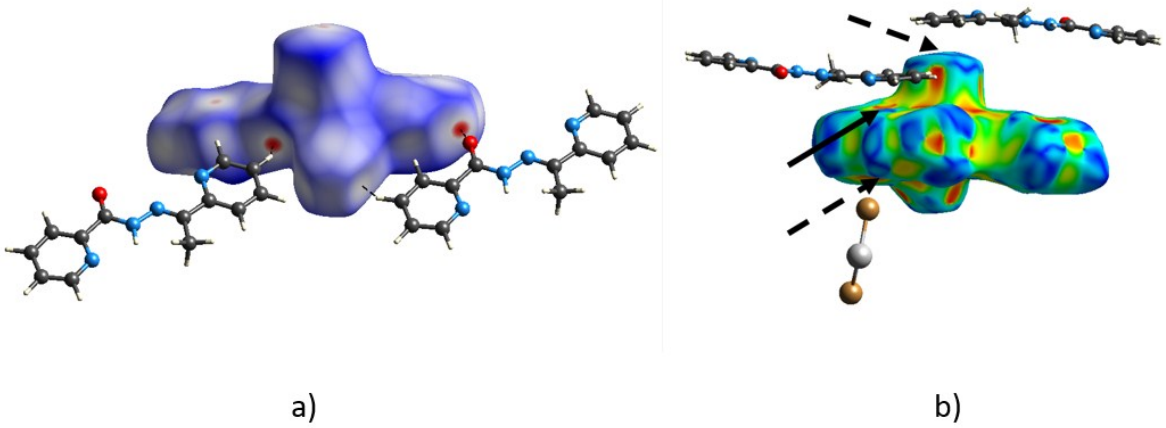

Fig. S5. Hirshfeld surface of **5** a) mapped with d_{norm} function with hydrogen bonds as dashed lines; b) mapped with shape index fuction. Plain arrow indicates 'bow-tie' patterns while dashed arrows indicate compatible parts of the HS.

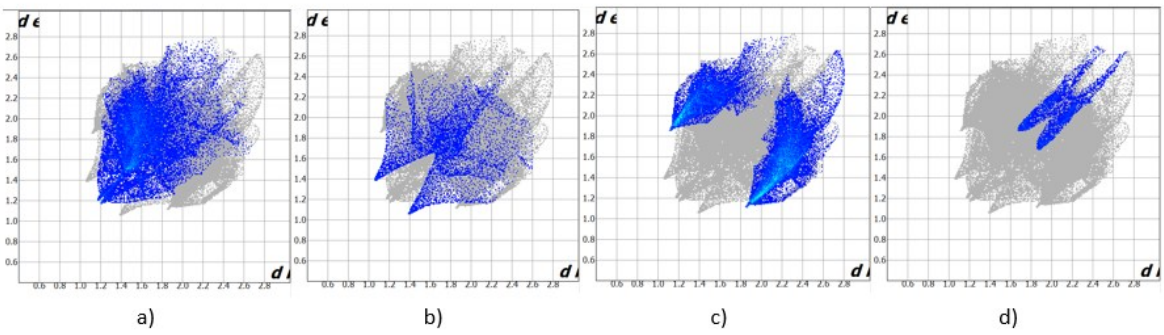

Fig. S6. Decomposed fingerprint plots of **5** a) H···H, b) H···O, c) H···Br, d) C···Br.

When Hirshfeld surface of **6** is mapped with d_{norm} function several red areas can be noticed. Eight large ones correspond to four major interactions between complex molecules. Four of the red spots are concentrated in a 'pocket' on one side of the Hirshfeld surface (Fig. S7a) with the other four on a complementary bulge on the other side of the surface. Three of the mentioned interactions are hydrogen bonds – one strong (N13-H13···O22) and two weak ones (C11-H11A···O22, C11-H11B···O22). The fourth interaction is presented as a short N···O contact (N17···O22, approximately 2.5Å). The hydrogen atom is not located, however the length of the contact suggest that it is a strong hydrogen bond with the hydrogen atom riding on the O22 atom. There are additional five small red spots on the HS. Three of them are due to presence of short C···C contacts (C18···C6, C6···C14) consistent with 'bow-tie' patterns which are evident on the surface mapped with shape index function (Fig. S7b), indicative of stacking interactions. Other two small red areas correspond to one weak C-H···I hydrogen bond (C6-H6···I3). Analysis of decomposed fingerprint plots (Fig S8) indicates that, unlike in the previous compounds, H···O contacts play a significant role (15.7% of the surface) in packing of the molecules.

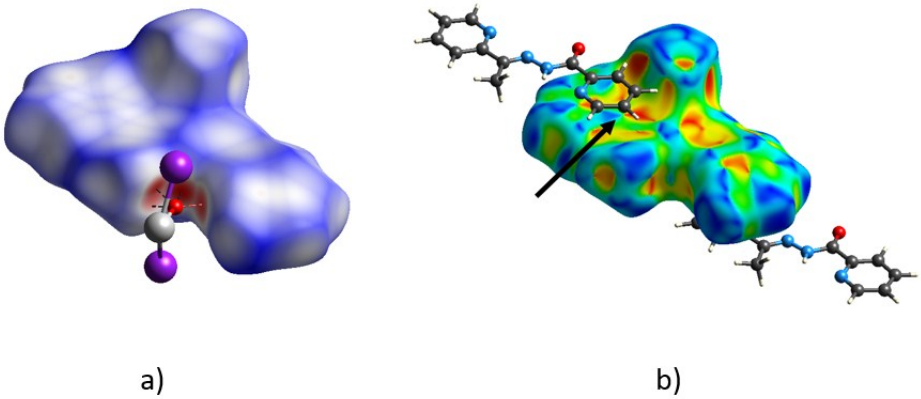

Fig. S7. Hirshfeld surface of **6** a) mapped with d_{norm} function; black dashed lined indicate hydrogen bonds, while red dashed line indicates close N···O contact; b) mapped with shape index function with 'bow-tie' patters marked with arrow.

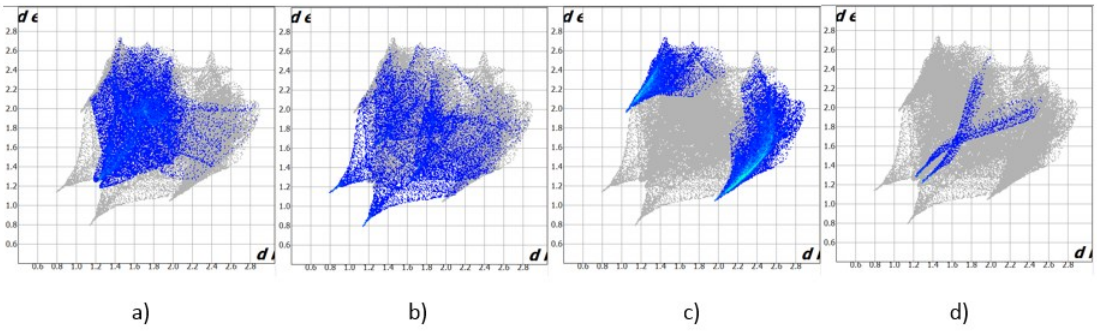

Fig. S8. Decomposed fingerprint plots of **6** a) H···H, b) H···O, c) H···I, d) N···O.

As with compound **7** (see main text) the Hirshfeld surface has been generated only for one complex molecule from two present in the asymmetric unit. Like in **7**, H···N decomposed plot is most obviously asymmetric, however lack of close H···N contact makes it less noticeable. Close H···O and H···Br contacts are manifested as twelve red areas on the surface mapped with d_{norm} function. Two of them are consistent with one C-H···O hydrogen bond (C056-H05D···O008, Fig. S9a) and the rest correspond to five C-H···Br interactions (C032-H03B···Br03, C024-H02A···Br04, C050-H05A···Br05, C042-H04B···Br03 and C034-H03C···Br05). Lastly one red spot is present due to a C-H···C contact (C024-H02A···C031). Application of shape index function reveals 'bow-tie' patterns typical for previously described compounds (Fig. S9b). Types of interactions contributing to packing of the molecules are the same as in most previous compounds - van der Waals forces (H···H, 31.9%) and interactions involving halogen ions (H···Br, 28.1%, Fig. S10).

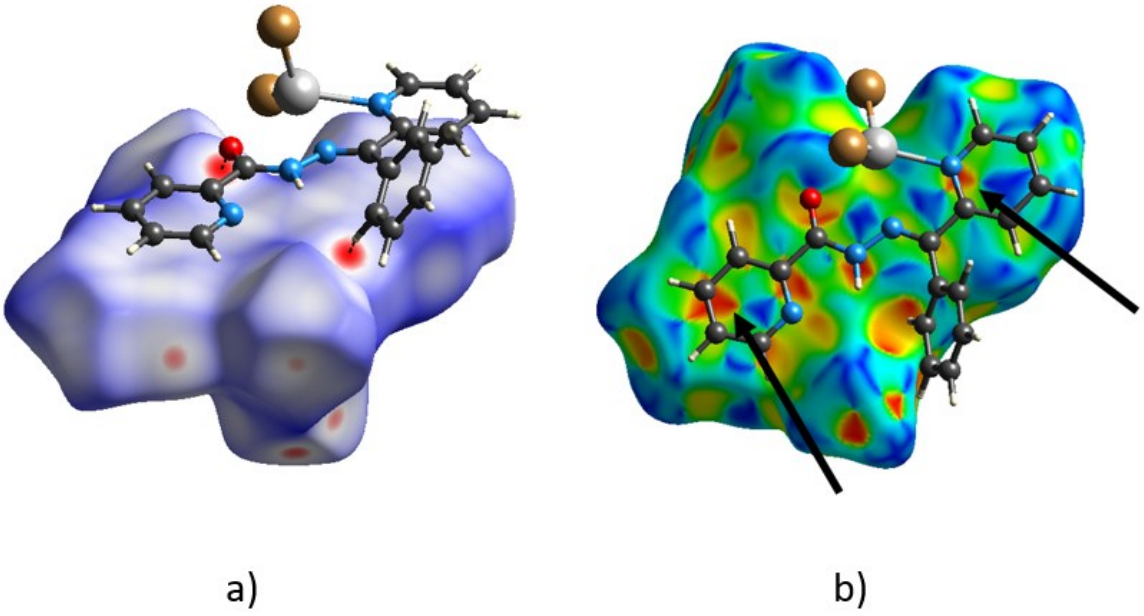

Fig. 9. Hirshfeld surface of **8** a) mapped with d_{norm} function with hydrogen bonds marked with dashed lines; b) mapped with shape index function; arrows mark 'bow-tie' patterns.

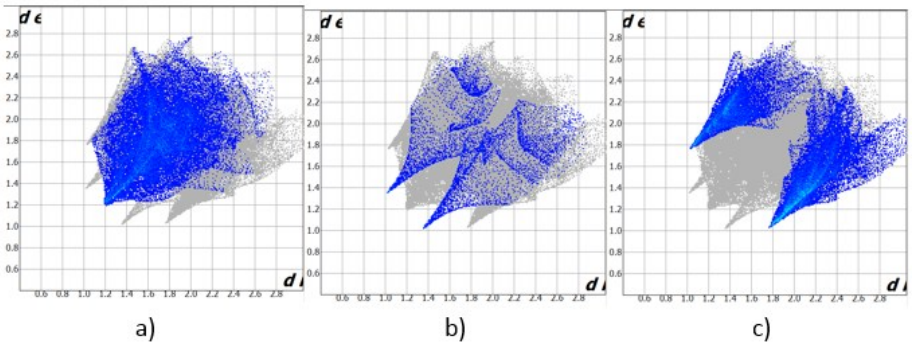

Fig. S10. Decomposed fingerprint plots of **8** a) H···H, b) H···O, c) H···Br.

The Hirshfeld surface of **9** mapped with d_{norm} function has very little interesting features. There are only three small red spots (Fig. S11a). They correspond to two C-H···O interactions (C007-H19···C036 and C036-H8···C063). Use of shape index function reveals typical 'bow-tie' patters (Fig. S11b), indicative of π···π stacking interactions between aromatic rings of adjacent molecules. As in previous compounds when decomposed fingerprint plots (Fig. S12) are considered, van der Waals forces (31.1%) and hydrogen···halogen interactions (27.1%) prove to contribute mostly to molecule packing in crystal.

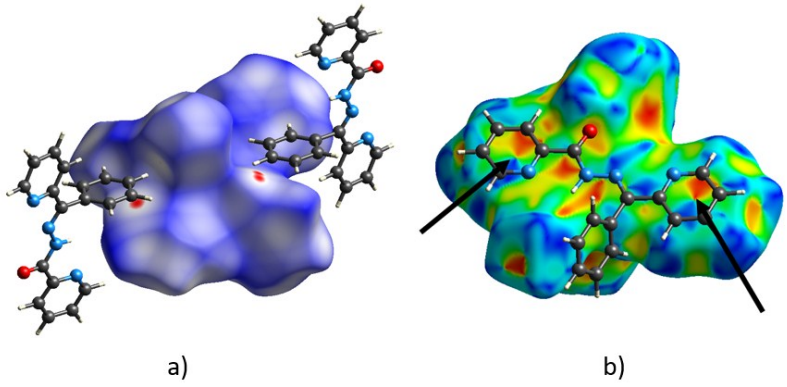

Fig. S11. Hirshfeld surface of **9** a) mapped with d_{norm} function; b) mapped with shape index function with arrows marking 'bow-tie' patterns.

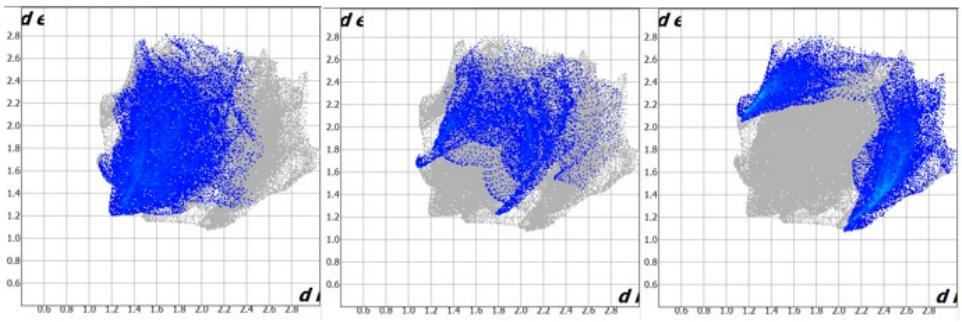

Fig. S12. Decomposed fingerprint plots of **9** a) H···H, b) H···C, c) H···I.

Contribution of specific types of contacts to the Hirshfeld surface in compounds **1-9** has been summarized in Fig. 16 (main text). As previously mentioned in all of the described compounds there are two types of dominant interactions: van der Waals forces (H···H contacts) and weak hydrogen bonds involving halogen ions (H···Halogen contacts). Additionally in case of compound **6** interactions involving oxygen atoms (strong hydrogen bonds) play an important role, as with C-H···π interactions (H···C contacts) in compounds **7**, **8** and **9**.